Optimization of population transfer by adiabatic passage

S. Guérin,* S. Thomas, and H. R. Jauslin
Laboratoire de Physique de l'Université de Bourgogne, CNRS, Boîte Postale, 47870, 21078 Dijon, France
(Received 13 July 2001; revised manuscript received 12 September 2001; published 15 January 2002)

We examine the adiabatic limit of population transfer in two-level models driven by a chirped laser field. We show that the nonadiabatic correction is minimized when the adiabatic eigenenergies associated to the dynamics are parallel. In the diagram of the difference of the eigenenergy surfaces as a function of the parameters, this corresponds to an adiabatic passage along a level line. The analytical arguments are based on the Dykhne-Davis-Pechukas treatment. We illustrate this behavior with various examples.

DOI: 10.1103/PhysRevA.65.023409 PACS number(s): 42.50.Hz, 32.80.Bx, 33.80.Be

I. INTRODUCTION

It is well known, since the prototype model of Landau and Zener [1,2], that two energy levels coupled by an appropriate time-dependent interaction can exchange population when they are brought through resonance adiabatically. The instantaneous eigenenergies as a function of time yield generally an avoided crossing that allows to describe the dynamics in the adiabatic regime [1–11]. In the context of the atom-laser interaction, this model describes a two-level atom driven by a pulsed laser field chirped around the one-photon resonance, in the rotating wave approximation [12,13]. Superadiabatic schemes introduced by Berry [6,14–16] have allowed us to study in detail the effect of the nonadiabatic corrections (see also, e.g., Refs. [17,18]). On the other hand, independently of any adiabatic condition, exact analytic solutions have been derived for specific classes of models [19–31]. The success of adiabatic passage to achieve population transfer between quantum states lies on the fact that a unique statevector is followed during the dynamics, which is continuously connected to the initial and final atomic eigenstates. Adiabatic passage has the advantage of robustness with respect to fluctuations and uncertainty of the parameters. A very important practical advantage is the insensitivity with respect to the pulse area. This is not so for the usual resonant "π-pulse" interaction (corresponding to half a Rabi cycle) with a constant resonant frequency, which requires a specific pulse area to reach the complete population transfer. In this case the dynamics can be analyzed as an initial projection on the two dressed eigenstates, followed by an adiabatic passage along these two branches of eigenstates, which interfere at the end of the pulse. The population transfer depends on a relative phase and is not robust with respect to the pulse area.

Geometrical tools have been developed to study the adiabatic passage: they allow to itemize qualitatively the possible connections between the quantum states of a given model [32,33]. We extend these geometrical tools to show that they also allow to design the *optimal* time-dependent parameters leading to robust population transfer.

We consider the eigenenergy surfaces as a function of the time-dependent parameters of the coupling. A contour plot of the difference of the eigenenergy surfaces exhibits *level lines*. The goal of this paper is to show for a class of models that *the passage along these level lines in the adiabatic regime minimizes the nonadiabatic correction and that it corresponds to the minimum pulse area that minimizes them*. The adiabatic criterion is thus reduced to the choice of a level line, corresponding to the choice of a chirp width.

In the next section, we establish the model and recall some well-known results. The third section is devoted to the proof of our statement with arguments based on the Dykhne-Davis-Pechukas formula. In Sec. IV and V we apply it to several examples. In Sec. VI, we discuss the incidence of counterrotating terms of a more realistic laser interaction on the obtained results and their domain of validity.

II. THE MODEL

We consider the scaled Schrödinger equation (setting $\hbar=1$)

$$i\frac{\partial}{\partial\tau}\phi(\tau)=T\mathsf{H}(\tau)\phi(\tau),\quad \phi(\tau)=\begin{bmatrix}\phi_1(\tau)\\ \phi_2(\tau)\end{bmatrix}\in\mathbb{C}^2, \tag{1}$$

with the scaled time $\tau=t/T$ and the model

$$\mathsf{H}(\tau)=\begin{bmatrix}-\Delta(\tau) & \Omega(\tau)\\ \Omega(\tau) & \Delta(\tau)\end{bmatrix},\quad \Delta,\Omega\in\mathbb{R}. \tag{2}$$

In the context of the one-photon atom-laser field interaction, in the rotating wave approximation (RWA), the off-diagonal coupling Ω characterizes half the one-photon Rabi frequency (proportional to the field amplitude) and the diagonal element Δ, the detuning from the one-photon resonance [12]. At each time, the unitary transformation

$$\mathsf{U}(\tau)=\begin{bmatrix}\cos[\theta(\tau)/2] & -\sin[\theta(\tau)/2]\\ \sin[\theta(\tau)/2] & \cos[\theta(\tau)/2]\end{bmatrix}, \tag{3}$$

with

$$\tan\theta(\tau)=-\frac{\Omega(\tau)}{\Delta(\tau)},\quad 0\leqslant\theta(\tau)<\pi, \tag{4}$$

diagonalizes the Hamiltonian $\mathsf{H}(\tau)$,

*Email address: sguerin@u-bourgogne.fr

$$\mathsf{U}^{\dagger}(\tau)\mathsf{H}(\tau)\mathsf{U}(\tau)=\begin{bmatrix}\mathcal{E}(\tau) & 0\\ 0 & -\mathcal{E}(\tau)\end{bmatrix}\equiv\mathsf{D}(\tau), \tag{5}$$

with

$$\mathcal{E}(\tau)=\sqrt{\Delta^2(\tau)+\Omega^2(\tau)}. \tag{6}$$

The Schrödinger equation can be rewritten as

$$i\frac{\partial}{\partial\tau}\psi(\tau)=\left[T\mathsf{D}(\tau)-i\mathsf{U}^{\dagger}(\tau)\frac{\partial}{\partial\tau}\mathsf{U}(\tau)\right]\psi(\tau),$$
$$=\begin{bmatrix}T\mathcal{E}(\tau) & i\gamma(\tau)\\ -i\gamma(\tau) & -T\mathcal{E}(\tau)\end{bmatrix}\psi(\tau), \tag{7}$$

in terms of the adiabatic states $\psi(\tau)=\mathsf{U}^{\dagger}(\tau)\phi(\tau)$, with the off-diagonal nonadiabatic coupling

$$\gamma(\tau)\equiv\frac{1}{2}\frac{d\theta(\tau)}{d\tau}=\frac{1}{2}\frac{\Omega(\tau)\dot{\Delta}(\tau)-\dot{\Omega}(\tau)\Delta(\tau)}{\Delta^2(\tau)+\Omega^2(\tau)}. \tag{8}$$

In the adiabatic limit, defined as $T\to\infty$, the nonadiabatic coupling γ can be neglected and the dynamics follows the adiabatic states.

We assume that the interaction starts and ends at the respective scaled times $\tau_i\to-\infty$ and $\tau_f\to\infty$, i.e., $\Omega(\tau\to\tau_i)=\Omega(\tau\to\tau_f)=0$. In order that the resonance is crossed, we also assume $\Delta(\tau_i)<0$ and $\Delta(\tau_f)>0$ implying $\theta(\tau_i)\to0^+$, i.e., the incoming adiabatic states are equal to the bares states: $\psi(\tau_i)=\phi(\tau_i)$, and $\theta(\tau_f)\to\pi^-$, i.e., the outgoing adiabatic states are equal to the bare ones up to an irrelevant geometrical phase [34] with interchanged labels

$$[\psi_1(\tau_f),\psi_2(\tau_f)]=[-\phi_2(\tau_f),\phi_1(\tau_f)]. \tag{9}$$

Thus the adiabatic passage along an adiabatic state corresponds to a complete transition in terms of the bare atomic states. The geometrical Berry phase is here π or 0 when the adiabatic following is, respectively, along the components $\psi_1(\tau)$ or $\psi_2(\tau)$. The fact that only these two possible geometrical phases appear comes from the fact that only two parameters are independently varied [34]. We assume the initial condition $[\phi_1(\tau_i)=1,\phi_2(\tau_i)=0]$. We study the final probability of no transition between bare states $P_1(\tau_f)\equiv|\phi_1(\tau_f)|^2$, which corresponds to the probability of transition between the adiabatic states. We refer to $P_1(\tau_f)$ as the final nonadiabatic correction. We have $P_1(\tau_f)\to0$ in the adiabatic limit.

We remark that, if $\Delta(\tau)=0$ for all time (exact resonance), we have $\gamma(\tau)=0$ and independently of any adiabatic condition the exact solution reads

$$|\phi_2(\tau_f)|^2=\sin^2\left[T\int_{\tau_i}^{\tau_f}d\tau\,\Omega(\tau)\right]. \tag{10}$$

Thus in exact resonance there is a direct dependence of the population transfer on the pulse area.

For a given model, we can define an adiabatic parameter that measures the degree of adiabaticity and for which a range of values yields in practice approximately complete transition. For example, for the Landau-Zener model, we have a constant coupling $\Omega(\tau)=\Omega_0$ and a linear chirp $\Delta(\tau)=\beta^2t$. The probability of no transition is [1,2] $P_1(\tau_f)=\exp(-\pi\alpha)$, where $\alpha=\Omega_0^2/\beta^2$ is the adiabatic parameter. Significant deviations have been shown to exist for modifications of this model (see, e.g., Ref. [9] and more recently Ref. [35]).

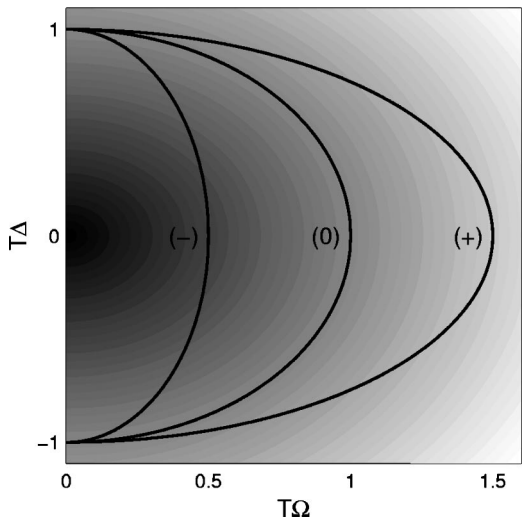

FIG. 1. Contour plot of the difference of the eigenenergies as a function of $T\Omega$ and $T\Delta$ (dimensionless). Three different paths with $T\Delta_0=1$ are shown: (0) is a level line; (–) and (+) are, respectively, paths below and above the level line (0).

In this paper, we look for a strategy to obtain the *optimal* population transfer with respect to the pulse area and to the chirp width, that takes into account the robustness of the process. We consider a process robust if significant local changes in the amplitude and form of the pulse and of the chirp do not change significantly the final transfer probability. In the strategies we choose the corrections come exclusively from nonadiabatic processes. For a given pulse shape, peak amplitude and chirp form, these corrections can be made arbitrarily small by taking long-enough pulses. We show that this optimal strategy consists in following a level line of the contour plot of the difference of the eigenenergy surfaces shown in Fig. 1.

III. OPTIMAL ADIABATIC PASSAGE

A. The dynamics in the parameter space

We analyze the final population transfer for different trajectories in the parameter space in the adiabatic limit. The trajectories are bounded: they start and end with finite values of the detuning $|\Delta(\tau_i)|=|\Delta(\tau_f)|=\Delta_0$. Figure 1 shows a contour plot of the difference of the eigenenergy surfaces as a function of the two scaled parameters $T\Omega$ and $T\Delta$. According to the eigenenergies (6), the contour plot displays level lines as half circles given by

$$\Omega^2+\Delta^2=\Delta_0^2, \tag{11}$$

with radius Δ_0 and center $\Omega=0$, $\Delta=0$. We are going to

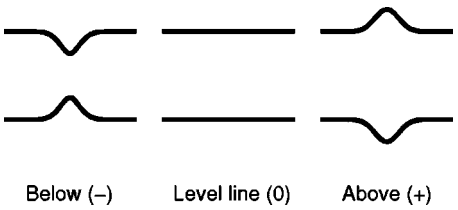

FIG. 2. Schematic eigenenergies as a function of time for the three typical paths (–), (0), and (+) of Fig. 1.

compare the transfer following the level lines given by circles with one-parameter families of other trajectories, that we choose to be ellipses. Three examples of trajectories are drawn in Fig. 1. The trajectory (0) is a level line. The trajectories (+) and (–) correspond to half ellipses of minor and major axis of respective length $2\Delta_0$ and $2\Omega_\pm$, centered in $\Omega=0$, $\Delta=0$, and of respective equation

$$\left(\frac{\Omega}{\Omega_\pm}\right)^2+\left(\frac{\Delta}{\Delta_0}\right)^2=1, \tag{12}$$

with $\Omega_-<\Delta_0<\Omega_+$. To parametrize these trajectories as a function of time, we assume a given smooth pulse shape $0\leqslant\Lambda(\tau)\leqslant 1$, maximum for $t=0$, related to the coupling by

$$\Omega(\tau)=\Omega_0\Lambda(\tau).$$

The detuning is then given by

$$\Delta(\tau)=\Delta_0 f(\tau), \tag{13}$$

with

$$f(\tau)=\frac{|\tau|}{\tau}\sqrt{1-\Lambda^2(\tau)}. \tag{14}$$

This parametrization implies

$$\mathcal{E}(\tau)=\sqrt{\Delta_0^2+(\Omega_0^2-\Delta_0^2)\Lambda^2(\tau)}. \tag{15}$$

For the trajectories (0), (−), and (+), we have thus, respectively, $\Omega_0=\Delta_0$, $\Omega_0=\Omega_-<\Delta_0$, and $\Omega_0=\Omega_+>\Delta_0$.

It is important to note that, since we assume that $\Lambda(\tau)$ has a maximum for $t=0$, the difference $2\mathcal{E}(0)$ of the eigenenergies at $t=0$ has a *minimum for the trajectories below the level line*, corresponding to an *avoided crossing* regime [trajectory (–)] and a *maximum for the trajectories above the level line*, corresponding to a two half-avoided-crossing regime [trajectory (+)] (see Fig. 2).

Although the choice of a one-parameter family of ellipses for comparison with the circular level lines is certainly not the most general one, it gives a simple and convenient way of illustrating the difference in transfer efficiency.

B. Optimization by the Dykhne-Davis-Pechukas formula

The Dykhne-Davis-Pechukas (DDP) formula [3–5] allows to calculate in the adiabatic asymptotic limit $T\to\infty$ the probability of the nonadiabatic transitions as an exponential decay. It reads in the simplest case

$$P_1(\tau_f)\rightsquigarrow\left|e^{iT\mathcal{D}(\tau_c)}\right|^2 \tag{16a}$$

$$\rightsquigarrow e^{-2T\,\mathrm{Im}\,\mathcal{D}(\tau_c)}, \tag{16b}$$

where

$$\mathcal{D}(\tau_c)=2\int_0^{\tau_c}d\tau\,\mathcal{E}(\tau) \tag{17}$$

is the integration of the analytic continuation of the difference of the eigenvalues up to τ_c, one of the complex *crossing points* of the eigenvalues defined by

$$\mathcal{E}(\tau_c)=0, \tag{18}$$

lying in the *upper* complex τ plane.

The criterion to choose the crossing point (which is not necessarily unique nor the closest one to the real axis, see below) has been established in Ref. [7] and for the cases where many crossing points are required, the formula (16a) has been generalized in Ref. [8]. The analysis is based on the *Stokes lines* defined as the set of points τ in the complex plane such that

$$\mathrm{Im}\,\mathcal{D}(\tau)=\mathrm{Im}\,\mathcal{D}(\tau_c)=\mathrm{const}. \tag{19}$$

An algorithm to construct numerically the Stokes line is described in the Appendix. The crossing points, denoted $\tau_c^{(n)}, n=1,N$, that one has to take into account are the ones connected by the Stokes line closest to the real axis. If there are several crossing points on this Stokes line, it has been shown [8] that one has to replace the term $e^{iT\mathcal{D}(\tau_c)}$ of formula (16a) by a coherent sum of exponentials, one for each crossing point connected by the lowest Stokes line,

$$P_1(\tau_f)\rightsquigarrow\left|\sum_{n=1}^{N}e^{iT\mathcal{D}[\tau_c^{(n)}]}\right|^2. \tag{20}$$

The required hypothesis [7,8] for the validity of this formula are (i) $\mathcal{E}(\tau)$ *does not vanish for real* τ (*e.g., no crossing at infinity) and* (ii) $\mathcal{E}(\tau)$*is analytic and single-valued throughout the region from the real axis to the relevant Stokes line*. We remark that for complex Hermitian Hamiltonians, with three time-dependent parameters, this formula has to be completed by geometrical prefactors [6,7].

In the cases we study [characterized by the quantity (15)], Eq. (18) gives

$$\Lambda(\tau_c)=\pm i\frac{\Delta_0}{\sqrt{\Omega_0^2-\Delta_0^2}}\quad\text{for }\Omega_0>\Delta_0, \tag{21a}$$

$$\Lambda(\tau_c)=\pm\frac{\Delta_0}{\sqrt{\Delta_0^2-\Omega_0^2}}\quad\text{for }\Omega_0<\Delta_0. \tag{21b}$$

When the eigenenergies are parallel (i.e., follow a level line $\Omega_0=\Delta_0$), we can calculate the limits of the transition points from above and from below a level line.

The DDP formula (20) indicates that the dominant nonadiabatic correction can be made to vanish

$$P_1(\tau_f) \rightsquigarrow 0, \tag{22}$$

in two different ways: (i) if each of the exponents in Eq. (20) tends to infinity, i.e.,

$$\mathrm{Im}\,\mathcal{D}[\tau_c^{(n)}] \to +\infty, \quad \text{for all } n, \tag{23}$$

or (ii) by destructive interference of the sum of nonzero exponents in Ref. (20).

We consider a particular type of pulse shapes given by entire analytic functions $\Lambda(\tau)$ that satisfy the condition

$$\Lambda(\tau) \to \infty \qquad \text{if and only if} \qquad \mathrm{Im}\,\tau \to \infty. \tag{24}$$

An example of this class of functions is the Gaussian pulse

$$\Lambda(\tau) = e^{-\tau^2} \tag{25a}$$

$$= e^{-(\mathrm{Re}\,\tau)^2} e^{(\mathrm{Im}\,\tau)^2} e^{-2i\,\mathrm{Re}\,\tau\,\mathrm{Im}\,\tau}. \tag{25b}$$

For this class of functions we can conclude using Eq. (21) that

$$|\Omega_0 - \Delta_0| \to 0 \qquad \text{if and only if} \qquad \mathrm{Im}\,\tau_c \to \infty \tag{26}$$

and further from Eqs. (17) and (15)

$$\lim_{|\Omega_0-\Delta_0|\to 0} \mathrm{Im}\,\mathcal{D}(\tau_c) = 2\,\mathrm{Im}\int_0^\infty d\tau \Delta_0^2 = \infty. \tag{27}$$

Therefore, from Eq. (20), we conclude that

$$\lim_{|\Omega_0-\Delta_0|\to 0} P_1(\tau_f) = 0, \tag{28}$$

i.e., for the class of pulse shapes satisfying Eq. (24) the dominant nonadiabatic correction given by the DDP formula (20) vanishes for the level lines.

This argument implies that (i) is achieved by the circular level lines:

Proposition A. Under the hypothesis that $\mathcal{E}(\tau)$ is entire and that for x real, there exist finite complex numbers z_+ and z_- independent of y such that, for all real y,

$$\lim_{x\to\pm\infty} \Lambda(x+iy) = z_\pm, \tag{29}$$

then

$$|\Omega_0 - \Delta_0| \to 0 \quad \text{if and only if} \quad \mathrm{Im}\,\mathcal{D}(\tau_c) \to +\infty. \tag{30}$$

We conclude that under the condition of Proposition A, *the level lines are optimal for adiabatic passage in the sense that they are the adiabatic path for which the nonadiabatic correction of the DDP formula vanish.*

We have already noticed that destructive interferences in Ref. (20) can also lead to vanishing dominant nonadiabatic correction. We will, however, see the following result: *the level lines correspond to the smallest pulse areas that make the dominant nonadiabatic correction vanish according to Eq. (30).*

This claim will be shown in some examples; it can be also intuitively seen as follows: Below the level lines $\Omega_0 < \Delta_0$, where the eigenenergies exhibit an avoided crossing, the relevant crossing point will be generically unique. The adiabatic regime will be better for higher pulse amplitude Ω_0 below the level lines. Above the level lines $\Omega_0 > \Delta_0$, where the eigenenergies exhibit a maximum, the relevant crossing points will be generically multiple and will lead to interferences. We can intuitively understand this fact, considering that the eigenenergies start and end in the middle of an avoided crossing (see Fig. 2). Thus in the adiabatic regime, the level lines $\Omega_0 = \Delta_0$ can be seen as a boundary between decreasing and oscillating regimes for the nonadiabatic correction. The minimum pulse area corresponding to the zero of the dominant nonadiabatic correction will be given for the adiabatic passage along a level line.

If $\mathcal{E}(\tau)$ has one finite singularity (or more), which we denote τ_s, the circular level lines $|\Omega_0 - \Delta_0| \to 0$ can imply that $\tau_c \to \tau_s$, from Eqs. (21). In this case, Proposition A does not hold. We will however see in Sec. IV, through examples, that the level lines will still characterize a boundary between decreasing and oscillating regimes for the nonadiabatic correction, and more importantly that *they still converge in the adiabatic limit to the first minimum of the nonadiabatic correction.*

The level lines can thus be seen as a *threshold characterizing a minimum pulse area beyond which we obtain efficient robust adiabatic passage.*

C. Estimation on the adiabatic regime: Choice of a level line

The nonadiabatic correction given by the DDP formula are valid in the adiabatic regime $T \to \infty$. In this section we discuss a rough determination of this adiabatic regime in terms of the parameters Ω, Δ of the model. We formulate a criterion that allows to determine the approximate extent of the adiabatic regime.

The analysis in terms of the DDP formula leads to the conclusion that at any level line the nonadiabatic transitions vanish. In this context all the level lines seem equivalent. There is, however, a clear difference among the level lines observed in the numerical simulations: level lines with small values of $\Delta_0 T = \Omega_0 T$ produce larger transition rates than the ones with large $\Delta_0 T = \Omega_0 T$ (see next sections). The difference can be attributed to the fact that if $\Delta_0 T = \Omega_0 T$ is small, then the system is far from the adiabatic regime, and the DDP formula does not give an accurate estimate of the corrections. The nonadiabatic (exponential) correction given by the DDP formula at the end of the pulse is beyond any power of $1/T$. We can, however, estimate the validity of the adiabatic regime that coincides with the validity of the DDP formula by making the first-order correction of the perturbation theory small.

First-order perturbation theory on the time-dependent Schrödinger equation (7) with respect to the small parameter $1/T$ gives approximately the correction, after integrating once by parts,

$$\left[\frac{\gamma(s)}{2T\mathcal{E}(s)}e^{-iT\int_{\tau_i}^{s}2\,du\,\mathcal{E}(u)}\right]_{\tau_i}^{\tau}. \tag{31}$$

Notice that if we consider the result at the end of the pulse, we are left with a correction including the initial and final first derivatives of the pulse. Higher-order terms involve successive derivatives of γ. Thus if the parameters $\Omega(\tau)$ and $\Delta(\tau)$ are not smooth at the early and final times, this gives the main contribution to the nonadiabatic correction [36–38].

Considering the intermediate times and the first-order perturbation theory (31), we thus take

$$\frac{|\gamma(\tau)|}{2T\mathcal{E}(\tau)} \ll 1 \tag{32}$$

as a characterization of the adiabatic regime.

On a level line, we have $\mathcal{E}(\tau)=\Delta_0, \Omega(\tau)\dot{\Omega}(\tau)+\Delta(\tau)\dot{\Delta}(\tau)=0$, which gives for $\Delta\neq 0$,

$$|\gamma(\tau)|=\left|\frac{\dot{\Omega}(\tau)}{2\Delta(\tau)}\right|=\frac{|\dot{\Lambda}(\tau)|}{2\sqrt{1-\Lambda^2(\tau)}}. \tag{33}$$

The condition (32) becomes

$$T\Delta_0 \gg \frac{|\dot{\Lambda}(\tau)|}{4\sqrt{1-\Lambda^2(\tau)}}. \tag{34}$$

Thus the adiabatic criterion (and the choice of a level line) is given by the condition (34).

IV. EXAMPLE WITH GAUSSIAN PULSES

We analyze in this section the Gaussian pulse

$$\Lambda_1(\tau)=e^{-\tau^2}, \tag{35}$$

which is entire and satisfies the conditions of Proposition A [for this pulse shape, the square root of Eq. (15) does not produce any branch point]. For comparison with the results of the next section, in the figures we use the normalized pulse area $\Omega_0 T\int_{-\infty}^{+\infty}d\tau\Lambda_1(\tau)/\pi=\Omega_0 T/\sqrt{\pi}$.

For $\Omega_0<\Delta_0$, the crossing points are given by

$$\sqrt{2}\,\tau_c^{(\pm,n)}=\pm\sqrt{\alpha_n-\beta}+i\sqrt{\alpha_n+\beta}, \tag{36}$$

with

$$\alpha_n=\sqrt{\beta^2+n^2\pi^2},\quad \beta=\ln\frac{\Delta_0}{\sqrt{\Delta_0^2-\Omega_0^2}}, \tag{37}$$

for n zero or a positive integer, and, for $\Omega_0>\Delta_0$, by

$$\sqrt{2}\,\tau_c^{(\pm,n)}=\pm\sqrt{\gamma_n+\delta}+i\sqrt{\gamma_n-\delta}, \tag{38}$$

with

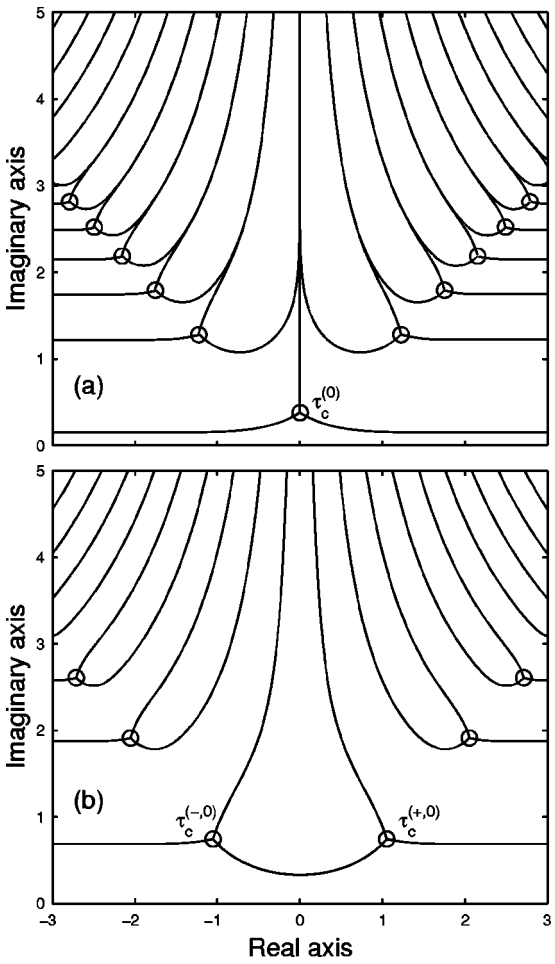

FIG. 3. Stokes lines in the complex plane of τ (dimensionless) for the Gaussian pulse shape: (a) for $\Omega_0/\Delta_0=1/2<1$ and (b) for $\Omega_0/\Delta_0=2>1$. The first crossing points are marked by circles.

$$\gamma_n=\sqrt{\delta^2+\left(2n-\frac{1}{2}\right)^2\pi^2},\quad \delta=\ln\frac{\sqrt{\Omega_0^2-\Delta_0^2}}{\Delta_0}. \tag{39}$$

The Stokes lines are displayed in Fig. 3. For $\Omega_0<\Delta_0$, the Stokes line closest to the real axis crosses the unique crossing point $\tau_c^{(0)}=i\sqrt{\beta}$. For $\Omega_0>\Delta_0$, the Stokes line closest to the real axis connects the two crossing points $\tau_c^{(\pm,0)}=\pm\sqrt{\gamma_0+\delta}+i\sqrt{\gamma_0-\delta}$. We can see that, denoting τ_c the relevant crossing point(s) on the Stokes line closest to the real axis, we have $\lim_{|\Omega_0-\Delta_0|\to 0}\mathrm{Im}\,\tau_c=+\infty$, which is in agreement with proposition A. We also have $\lim_{|\Omega_0-\Delta_0|\to 0}\mathrm{Re}\,\tau_c=0$. (These two last results are also true for all the other crossing points $\tau_c^{(\pm,n)}$.)

Figure 4 shows the contour plot of $\log[P_1(\tau_f)]$ as a function of $T\Delta_0$ and $T\Omega_0/\sqrt{\pi}$. We can observe for $\Delta_0=0$ (no chirp and zero detuning) oscillations of the population between 0 and 1, which correspond to the well-known Rabi oscillations. In this model (2), the complete population transfer occurs exactly when Ω_0 satisfies

$$T\Omega_0\int_{-\infty}^{+\infty}\Lambda(\tau)d\tau=\left(k+\frac{1}{2}\right)\pi,\quad k\ \text{integer}, \tag{40}$$

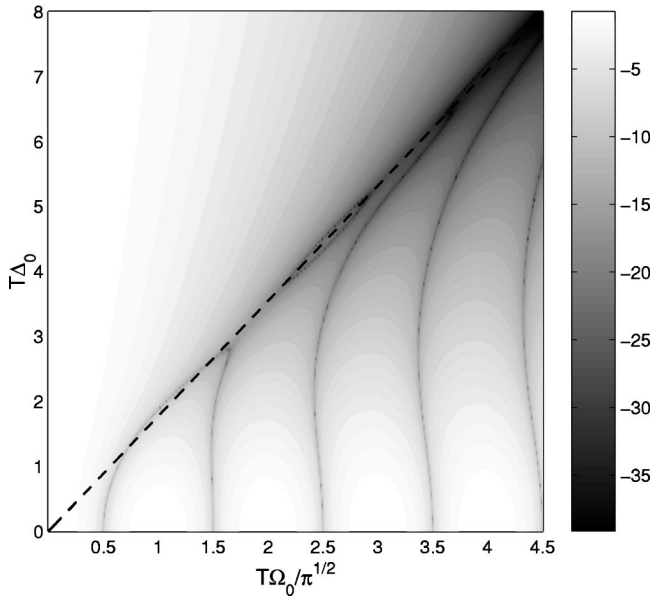

FIG. 4. For the Gaussian pulse shape, contour map of natural logarithm of the nonadiabatic corrections at the end of the pulse $\log[P_1(\infty)]$ as a function of the normalized pulse area $T\Omega_0/\sqrt{\pi}$ and the chirp widths $T\Delta_0$ (dimensionless). Darker points correspond to smaller $P_1(\infty)$. The dashed line corresponds to the level lines $\Delta_0=\Omega_0$.

according to Eq. (10). However, this population transfer is not robust with respect to the pulse area as can be seen by the strong gradients of the population along $\Delta_0=0$ for the (dark) values of Ω_0 satisfying Eq. (40).

We remark that the contour lines emerging almost vertically from $\Delta_0=0$ can be interpreted as follows: for a given pulse area, the robustness is quite good with respect to Δ_0, close to $\Delta_0=0$, in this model.

The Rabi oscillations extend continuously for $\Delta_0\neq 0$ with a larger width for larger $T\Delta_0$. For larger $T\Delta_0$, these oscillations become closer to zero in a large region: this corresponds to the robust almost complete population transfer of the adiabatic regime. As expected from Proposition A, the line of minimum $P_1(\tau_f)$ converges very fast in the adiabatic limit $T\rightarrow+\infty$ to the level lines $\Omega_0=\Delta_0$. We remark that the minimum pulse area leading to the (nonrobust) transfer is obtained for $\Delta_0=0$ with $k=0$ in Eq. (40).

It is important to note that *the level lines appear as a boundary between decreasing and oscillatory regimes for the nonadiabatic correction* $P_1(\tau_f)$, as shown by Fig. 4. This can be explained precisely by the two relevant crossing points occurring for $\Omega_0>\Delta_0$ as follows. Using the fact that $\mathcal{E}(\tau)$ is even with respect to the imaginary part of τ, we can calculate that

$$\mathrm{Im}\,\mathcal{D}[\tau_c^{(+)}]=\mathrm{Im}\,\mathcal{D}[\tau_c^{(-)}], \tag{41a}$$

$$\mathrm{Re}\,\mathcal{D}[\tau_c^{(+)}]\neq\mathrm{Re}\,\mathcal{D}[\tau_c^{(-)}]\neq 0, \tag{41b}$$

implying an oscillatory behavior for $\Omega_0>\Delta_0$,

$$P_1(\tau_f)\rightsquigarrow e^{-2T\,\mathrm{Im}\,\mathcal{D}[\tau_c^{(+)}]}\left|e^{iT\,\mathrm{Re}\,\mathcal{D}[\tau_c^{(+)}]}+e^{iT\,\mathrm{Re}\,\mathcal{D}[\tau_c^{(-)}]}\right|^2. \tag{42}$$

We also remark that, since we have $|\mathrm{Re}\,\mathcal{D}[\tau_c^{(+)}]|\neq|\mathrm{Re}\,\mathcal{D}[\tau_c^{(-)}]|$, the maximum of the oscillations depends on Ω_0, as seen on the contour plot in Fig. 4.

For $\Omega_0<\Delta_0$ the single transition point implies the probability with the exponential decay rate:

$$P_1(\tau_f)\rightsquigarrow e^{-2T\,\mathrm{Im}\,\mathcal{D}(\tau_c)}. \tag{43}$$

For this pulse shape, the adiabatic criterion (34) on the level lines $\Omega_0=\Delta_0$ is

$$T\Delta_0\gg\frac{1}{2\sqrt{2}}\approx 0.35. \tag{44}$$

We remark that the numerical results are in good agreement with the adiabatic estimates for quite small values of $T\Delta_0$.

To illustrate this criterion, we compare the robustness for the level line $T\Delta_0=T\Omega_0=1.75=5\times 0.35$ [which satisfies quite well the adiabatic criterion (44)] with the result for $\Delta_0=0$ (without chirp) for which the complete transfer occurs for $T\Omega_0\approx 0.886$ [Eq. (40)]. Along the level line, we obtain $P_1(+\infty)\approx 0.0015$. If we now add an error of 15% on the pulse-peak amplitude, it leads for $\Delta_0=0$ to a loss $P_1(+\infty)\approx 0.054$ [using Eq. (10)]. If we follow the level line ($T\Delta_0=T\Omega_0=1.75$) with the same error on the pulse-peak amplitude, it leads to the loss $P_1(+\infty)\approx 0.01$. Thus with an error of 15% on the pulse-peak amplitude, the loss is five times smaller on the level line than for $\Delta_0=0$ for an amplitude only twice bigger.

V. EXAMPLES WITH COMPLEX SINGULARITIES

We analyze in this section different pulse shapes that do not satisfy the conditions of Proposition A because they have singularities: (i) secant hyperbolic, (ii) Lorentzian, and (iii) sine squared,

$$\text{(i)}\quad \Lambda_2(\tau)=\mathrm{sech}(\tau), \tag{45a}$$

$$\text{(ii)}\quad \Lambda_3(\tau)=\frac{1}{1+\tau^2}, \tag{45b}$$

$$\text{(iii)}\quad \Lambda_4(\tau)=\sin^2(\pi\tau)\quad \text{for } 0\leqslant\tau\leqslant 1, \tag{45c}$$

$$=0\ \text{elsewhere}. \tag{45d}$$

The first two have singularities in the complex plane and thus proposition A is not applicable. The last one is not real analytic so that the DDP formula does not apply. In order to compare the effect of these different pulses, the figures are plotted with the normalized pulse area $\Omega_0 T\int_{-\infty}^{+\infty}d\tau\Lambda_j(\tau)/\pi$. [We have $\int_{-\infty}^{+\infty}d\tau\,\mathrm{sech}(\tau)=\pi$, $\int_{-\infty}^{+\infty}d\tau/(1+\tau^2)=\pi$, and $\int_0^1 d\tau\sin^2(\pi\tau)=1/2$.]

A. Secant hyperbolic pulse shape

The secant hyperbolic coupling shape $\Lambda_2(\tau)=\mathrm{sech}(\tau)$ [which leads to $f(\tau)=\tanh(\tau)$] does not satisfy the conditions of Proposition A since it contains singularities located at

$$\tau_s^{(n)}=i\pi\left(n+\frac{1}{2}\right), \tag{46}$$

for n zero or a positive integer. For $\Omega_0<\Delta_0$, the crossing points are all along the imaginary axis,

$$\tau_c^{(\pm,n)}=i\left[\pi\left(n+\frac{1}{2}\right)\pm\arcsin\frac{\sqrt{\Delta_0^2-\Omega_0^2}}{\Delta_0}\right], \tag{47}$$

and for $\Omega_0>\Delta_0$ they appear as pairs perpendicularly to the real axis,

$$\tau_c^{(\pm,n)}=\pm\,\mathrm{arsinh}\frac{\sqrt{\Omega_0^2-\Delta_0^2}}{\Delta_0}+i\pi\left(n+\frac{1}{2}\right). \tag{48}$$

The crossing points and the Stokes lines are displayed in Fig. 5. For $\Omega_0>\Delta_0$, the closest Stokes line to the real axis connects the two crossing points $\tau_c^{(\pm,0)}$. For $\Omega_0<\Delta_0$, the closest Stokes line to the real axis connects the two crossing points $\tau_c^{(-,0)}$ and $\tau_c^{(+,0)}$, however, *through the singularity* $\tau_s^{(0)}$. Because of this singularity, only the crossing point $\tau_c^{(-,0)}$ below it is taken into account. We can calculate the result of the DDP formula (20) in the adiabatic limit $T\to+\infty$,

$$P_1(\tau_f)\rightsquigarrow\exp[-2\pi T(\Delta_0-\sqrt{\Delta_0^2-\Omega_0^2})]\quad\text{for}\quad\Omega_0<\Delta_0, \tag{49a}$$

$$P_1(\tau_f)\rightsquigarrow 4\,\cos^2(\pi T\sqrt{\Omega_0^2-\Delta_0^2})e^{-2\pi T\Delta_0}\quad\text{for}\quad\Omega_0>\Delta_0. \tag{49b}$$

These results are compatible with the known exact results (for any regime, adiabatic or not) [20,25]

$$P_1(\tau_f)=\cosh^2(\pi T\sqrt{\Delta_0^2-\Omega_0^2})\,\mathrm{sech}^2(\pi\Delta_0 T). \tag{50}$$

For the level lines $\Omega_0=\Delta_0$, all the crossing points tend to the singularities by pairs

$$\lim_{|\Omega_0-\Delta_0|\to 0}\tau_c^{(\pm,n)}=\tau_s^{(n)}. \tag{51}$$

The result of the nonadiabatic correction can be found in this case by the formula (49b) in the limit $\Omega_0\to\Delta_0$,

$$P_1(\tau_f)\rightsquigarrow 4e^{-2\pi\Delta_0 T}. \tag{52}$$

We remark that the formula (49a) in the limit $\Omega_0\to\Delta_0$ does not give the correct limit. It is, however, correct if, instead of taking the closest crossing point to the real axis, below the singularity, the (two) closest ones *connected with the same Stokes lines* are taken into account in the DDP formula (20) [9]. We have indeed noticed numerically that the Stokes lines between the two crossing points $\tau_c^{(-,0)}$ and $\tau_c^{(+,0)}$ can be joined as if the singularity was ignored.

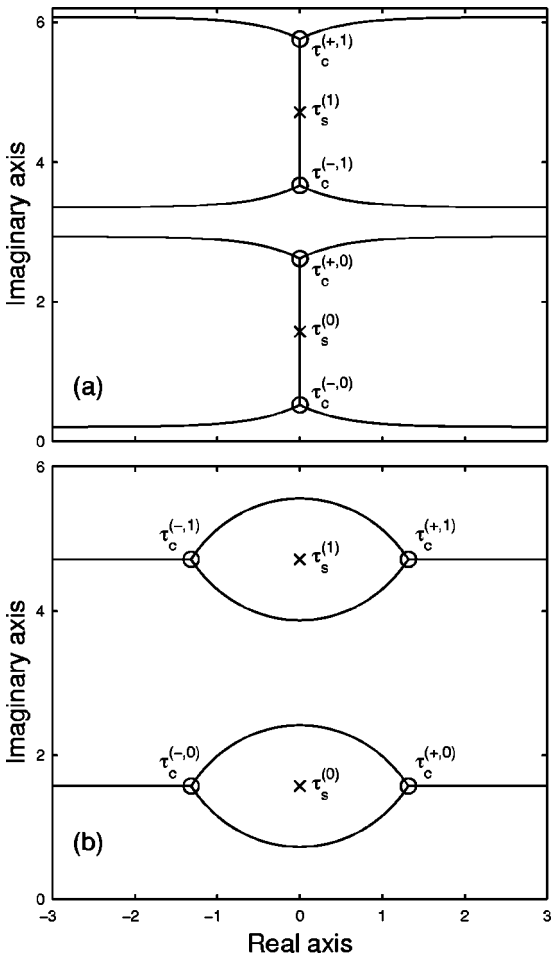

FIG. 5. The first Stokes lines in the complex plane of τ for the secant hyperbolic pulse shape: (a) for $\Omega_0/\Delta_0=1/2<1$ and (b) for $\Omega_0/\Delta_0=2>1$. The first singularities and crossing points are, respectively, shown with crosses and circles.

The results are collected in the contour plot of $\log[P_1(\tau_f)]$ as a function of $T\Delta_0$ and $T\Omega_0$ in Fig. 6. The qualitative aspects of this contour plot are very similar to the one obtained for the Gaussian pulse. From the preceding formulas of $P_1(\tau_f)$, we can clearly recover the two regimes already noticed for the exponential pulse: a nonoscillatory regime for $\Omega_0<\Delta_0$, followed by an oscillatory regime for $\Omega_0>\Delta_0$, with the boundary given by the level lines $\Omega_0=\Delta_0$. The optimal transition occurs for $\Omega_0>\Delta_0$, when the cosine of Eq. (49b) becomes zero, more precisely when

$$\Omega_0^2=\Delta_0^2+\frac{1}{T}\left(\frac{1}{2}+n\right)^2,\quad n\ \text{integer}, \tag{53}$$

which in the adiabatic limit $T\to\infty$ becomes

$$\Omega_0=\Delta_0. \tag{54}$$

The optimal transition occurs thus again along a level line in the adiabatic limit. The criterion (34) for a level line to be optimal becomes here

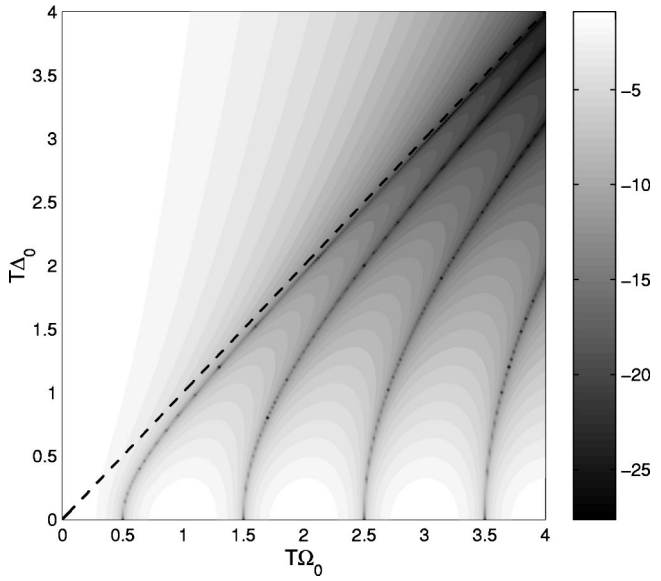

FIG. 6. For the secant hyperbolic pulse shape, contour map of $\log[P_1(\infty)]$.

$$T\Delta_0 \gg 1/4. \tag{55}$$

Figure 6 shows that the lines of $P_1(\tau_f)$ converge less fast to the level lines $\Omega_0=\Delta_0$ than for the exponential shape. We remark that Eq. (53) shows that for a given finite $T\Delta_0$ the level lines always underestimate the optimal value of $T\Omega_0$.

We can also see that for a given pulse area $\Omega_0 T\int_{-\infty}^{+\infty} d\tau \Lambda_j(\tau)$, the transfer is more efficient for the secant hyperbolic pulse than for the Gaussian pulse in the sense that the same transfer is obtained for a lower Δ_0. On the other hand, for a given chirp width Δ_0, the transfer is less efficient than for the Gaussian pulse in the sense that the same transfer is obtained for a larger pulse area. These two preceding remarks can be easily explained by the facts that the pulse area is smaller for the Gaussian pulse and that the level lines $\Delta_0=\Omega_0$ depend on pulse peak amplitudes and not on pulse areas.

B. Lorentzian shape

The Lorentzian coupling shape $\Lambda_3(\tau)=1/(1+\tau^2)$ contains one singularity in the upper complex τ plane, located at

$$\tau_s = i.$$

The crossing points are double for $\Omega_0<\Delta_0$,

$$\tau_c^{(\pm)} = i\left(1 \pm \sqrt{1-\frac{\Omega_0^2}{\Delta_0^2}}\right), \tag{56}$$

and for $\Omega_0>\Delta_0$,

$$\sqrt{2}\,\tau_c^{(\pm)} = \pm\sqrt{\frac{\Omega_0}{\Delta_0}-1} + i\sqrt{\frac{\Omega_0}{\Delta_0}+1}. \tag{57}$$

The Stokes lines are displayed in Fig. 7.

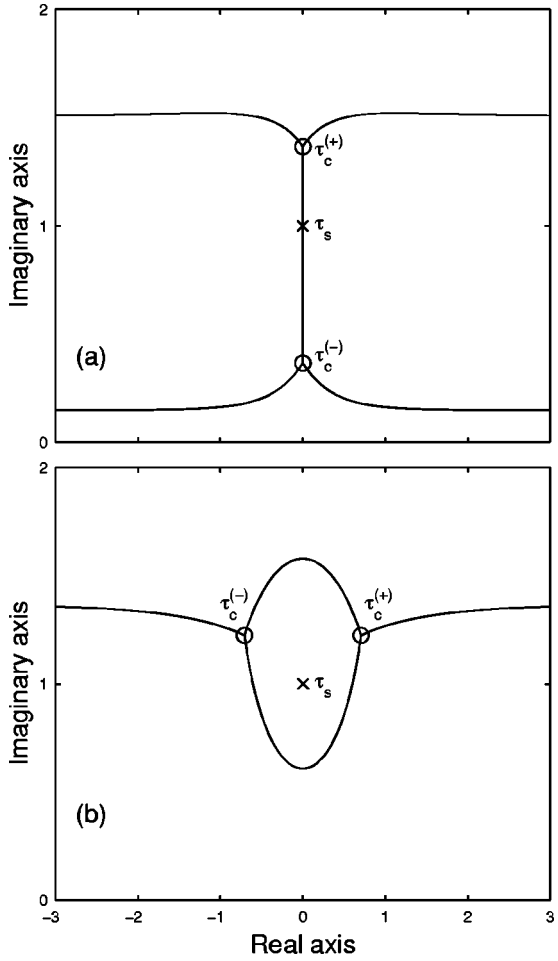

FIG. 7. The Stokes lines in the complex plane of τ for the Lorentzian pulse shape: (a) for $\Omega_0/\Delta_0=1/2<1$ and (b) for $\Omega_0/\Delta_0=2>1$. In each case, the singularity and the crossing points are, respectively, shown with a cross and circles.

We see that, like for the secant hyperbolic shape, for the level lines $|\Omega_0-\Delta_0|\to 0$, the crossing points go to the singularity of $\Lambda_2(\tau)$. We do not have known solutions for this case. We obtain along a level line

$$\lim_{|\Omega_0-\Delta_0|\to 0} \mathrm{Im}\,\mathcal{D}(\tau_c) = 2\Delta_0, \tag{58}$$

which, taking into account the two crossing points $\tau_c^{(\pm)}$ joined by the Stokes line through the singularity as for the secant hyperbolic pulse, leads to

$$P_1(\tau_f) \rightsquigarrow 4e^{-4\Delta_0 T}. \tag{59}$$

We note that $P_1(\tau_f)$ is less favorable than for the secant hyperbolic shape [to be compared with the formula (52)].

As with the two preceding cases, we have the oscillatory and nonoscillatory regimes separated by the level lines $\Omega_0=\Delta_0$ in Fig. 8 of the contour plot of $P_1(\tau_f)$. The first minimum line of $P_1(\tau_f)$ converges to the level lines: *the level lines give again here the optimal transfer in the adiabatic limit.*

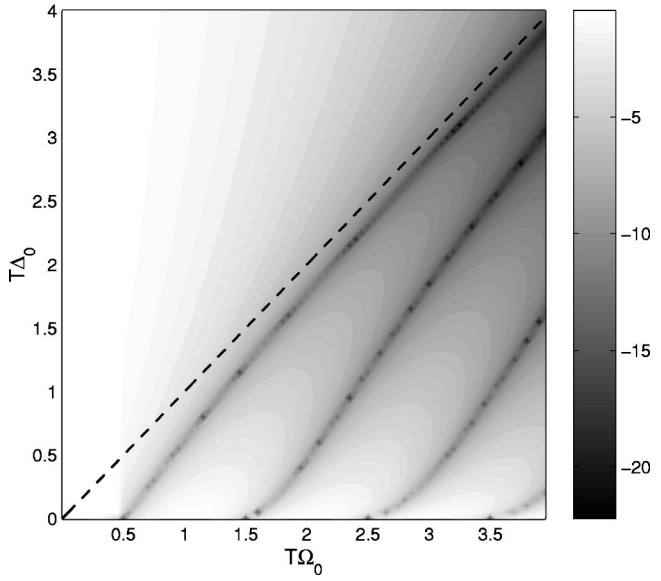

FIG. 8. For the Lorentzian pulse shape, contour map of $\log[P_1(\infty)]$.

For this shape, the adiabaticity criterion (34) on the level lines is

$$T\Delta_0 \gg \frac{1}{2\sqrt{2}} \approx 0.35, \tag{60}$$

which is more restricitive than for the secant hyperbolic pulse.

C. Sine-squared shape

The sine-squared coupling shape $\Lambda_4(\tau)=\sin^2(\pi\tau)$ is not real analytic and the DDP analysis does not apply. Figure 9 shows the contour plot of $P_1(\tau_f)$ as a function of $T\Delta_0$ and $T\Omega_0/(2\pi)$. The minimum of probability $P_1(\tau_f)$ does not converge to the level lines $\Omega_0=\Delta_0$, which thus have no particular sense in this case. In fact, the nonadiabatic correction, as explained in Sec. III C is given by the nonsmoothness of the pulse ends, which, in this example, is characterized by discontinuous second derivatives. Thus, the nonadiabatic correction $P_1(\tau_f)$ is of order $1/T^4$ in the adiabatic limit $T\rightarrow\infty$. We can estimate it more precisely along the level lines $\Omega_0=\Delta_0$ using the first-order perturbation theory as described in Sec. III C. We obtain approximately after integrating twice by parts

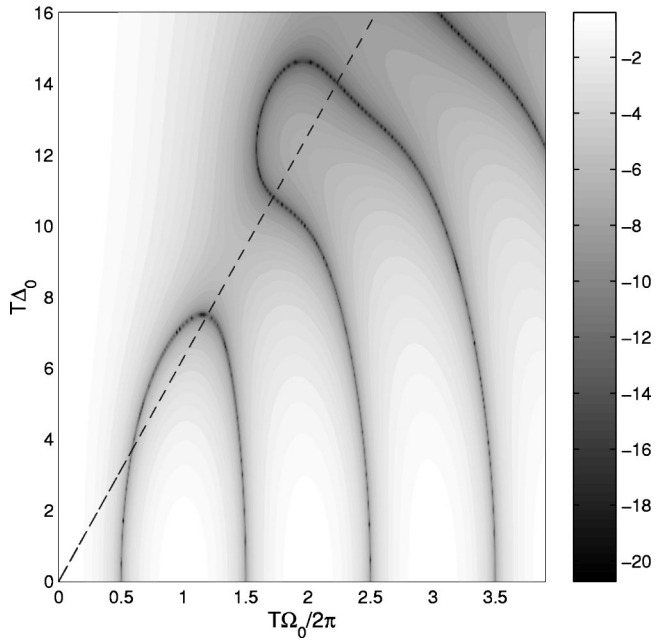

FIG. 9. For the sine-squared pulse shape, contour map of $\log[P_1(\infty)]$.

$$P_1(\tau_f) \rightsquigarrow \frac{1}{4}\left(\frac{\pi}{T\Omega_0}\right)^4 \sin^2(\Omega_0 T), \tag{61}$$

which fits quite accurately the nonadiabatic corrections along the level lines for large $\Omega_0 T$.

VI. EFFECT OF THE COUNTERROTATING TERM OF A LASER–TWO-LEVEL-ATOM INTERACTION

In this section we study a two-level atom interacting with a pulsed and chirped laser field, taking into account the counterrotating term. The Hamiltonian, associated with the Schrödinger equation (1), is in this case

$$\mathsf{H}(\tau)=\frac{\omega_0}{2}\begin{bmatrix}-1 & 0\\ 0 & 1\end{bmatrix}+\frac{\mu E(\tau)}{\hbar}\cos\phi(\tau)\begin{bmatrix}0 & 1\\ 1 & 0\end{bmatrix}, \tag{62}$$

with the atomic Bohr frequency ω_0, the dipole moment μ, the electric-field envelope $E(\tau)$ and its phase $\phi(\tau)$. After a time-independent unitary transformation that does not change the probabilities, it can be rewritten as a sum of the RWA Hamiltonian (2) and a ''counterrotating'' Hamiltonian

$$\mathsf{H}(\tau)=\begin{bmatrix}-\Delta(\tau) & \Omega(\tau)\\ \Omega(\tau) & \Delta(\tau)\end{bmatrix}+\Omega(\tau)\begin{bmatrix}0 & \exp\left\{-2iT\left[\omega_0\tau-2\int_{\tau_i}^{\tau}ds\,\Delta(s)\right]\right\}\\ \exp\left\{2iT\left[\omega_0\tau-2\int_{\tau_i}^{\tau}ds\,\Delta(s)\right]\right\} & 0\end{bmatrix}, \tag{63}$$

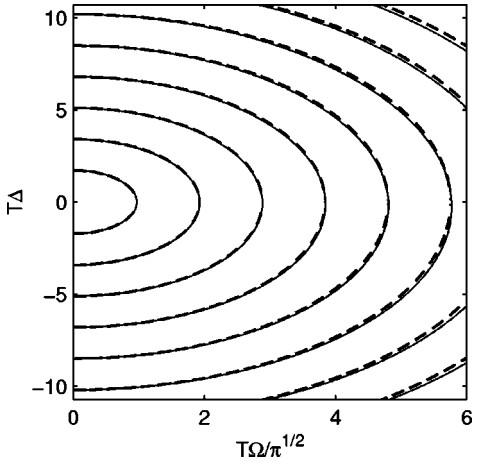

FIG. 10. Level lines (full lines) associated to the eigenvalues (66), for $\omega_0 T=50$, compared with the circles [as dashed lines, level lines of the RWA Hamiltonian (2)] .

with the effective detuning

$$2\Delta=\omega_0-\dot{\phi}, \tag{64}$$

and the Rabi frequency $2\Omega(\tau)=\mu E(\tau)/\hbar$. The dressed eigenelements in strong fields can be obtained from the Floquet Hamiltonian (see, for example, Refs. [39,40]). The DDP formula does not apply but we claim that the level lines stay relevant to optimize the adiabatic passage. If the counterrotating term is sufficiently strong (for example, such that dynamical resonances appear [40]), the level lines are strongly modified and are not circles anymore. In this section, we restrict the analysis of the effect of this counterrotating term on the optimality of the level line as circles, in the standard RWA limit

$$\Omega,\Delta\ll\omega_0, \tag{65}$$

and show that in this RWA limit the level line as circles are still a good strategy for the control of population transfer.

In the limit (65), we can calculate the dressed eigenvalues by perturbation theory [39]:

$$\lambda_{\pm}(\tau)\approx\pm\mathcal{E}(\tau)\mp\frac{\Omega^2(\tau)}{4\omega_0^2}\,\frac{\mathcal{E}^2(\tau)-2\Delta(\tau)\omega_0}{\mathcal{E}(\tau)}. \tag{66}$$

The level lines associated to these eigenvalues, i.e., the trajectories in the space parameter (Ω,Δ) such that $\lambda_+-\lambda_-=$const. are displayed in Fig. 10. From these eigenvalues (66), we can deduce the condition to recover level lines as circles

$$(T\Omega_0)^2\ll 2T\omega_0. \tag{67}$$

Thus we anticipate that the DDP analysis of the previous sections is still valid, i.e., that the level lines as circles optimize the population transfer by adiabatic passage, when the condition (67) is satisfied. This is checked numerically in Fig. 11 where contour plots of the nonadiabatic correction with the counterrotating term ($T\omega_0=50$) are drawn for the

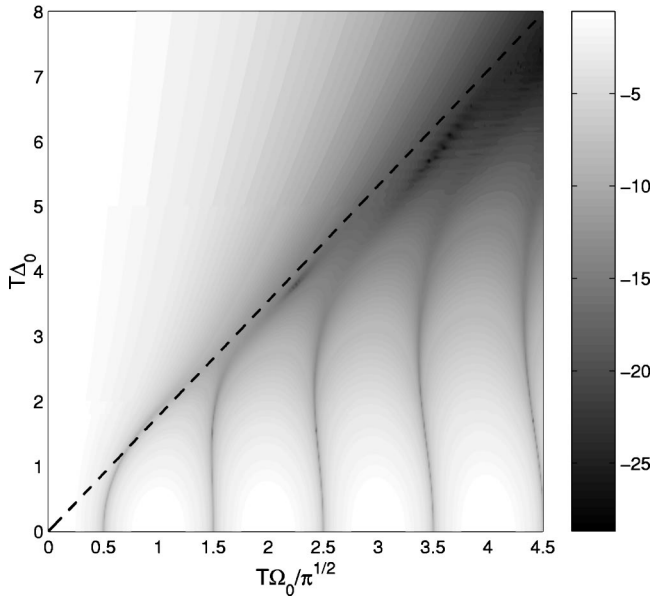

FIG. 11. For the Gaussian pulse shape, contour map of $\log[P_1(\infty)]$ with the counterrotating term, for $\omega_0 T=50$. To be compared with Fig. 4.

Gaussian pulses (described in Sec. IV) and with the ''ellipse'' dynamics described in Sec. III A. We can see that for the level lines satisfying $T\Omega_0\gtrsim 1/(2\sqrt{2})\approx 0.35$ [see, Eq. (44)] (say $T\Omega_0/\sqrt{\pi}\gtrsim 5\times 0.35/\sqrt{\pi}\approx 1$) can be still considered as optimal if Eq. (67) is also satisfied (say $T\Omega_0/\sqrt{\pi}\lesssim\sqrt{2T\omega_0/5}/\sqrt{\pi}\approx 2.5$).

VII. DISCUSSIONS AND CONCLUSIONS

We have demonstrated that for models with an entire analytic pulse shape, the first minimum of the nonadiabatic correction $P_1(\tau_f)\to 0$ is obtained in the adiabatic limit when the dynamics follows a level line $\Omega_0=\Delta_0$ in the parameter space. We have shown with the example of an exponential pulse that this first minimum converges very fast to the level line.

For a given pulse shape, the choice of the level line, corresponding to the choice of the chirp width $2\Delta_0$, has been estimated with perturbative arguments. For pulses having complex singularities, the demonstration is not valid. We have, however, shown analytically with the examples of secant hyperbolic and numerically with the Lorentzian pulses that the level line $\Omega_0=\Delta_0$ still converge to the first minimum of the nonadiabatic correction, however, with a slower convergence than for the exponential pulse. This result can be interpreted with the Dykhne-Davis-Pechukas formula. We have indeed shown that this formula implies for these examples that the level lines are the boundary between regions of a monotonic decreasing and of oscillations of $P_1(\tau_f)$. Thus for a given width of chirping, the level line gives the minimal pulse amplitude to be used to have complete transfer by adiabatic passage: Larger pulse amplitudes do not improve significantly the robust transfer. We also have characterized the regime of validity of our analysis for a more realistic laser interaction including a counterrotating term.

In conclusion, we have shown that for two-level models the optimal adiabatic passage occurs along a level line in the diagram of the difference of the eigenenergies as a function of the parameters. For problem with N-level systems, this result could be applied locally to design optimal time-dependent parameters to achieve selective robust adiabatic transfer.

ACKNOWLEDGMENTS

We thank A. Joye for many fruitful discussions and for providing us an efficient algorithm to construct the Stokes lines. We also thank N. Vitanov for useful comments.

APPENDIX: ALGORITHM FOR THE STOKES LINES

In this appendix, we present the method used to determine the Stokes lines. Stokes lines are defined as the set

$$\left\{ z \equiv x+iy \,\middle|\, \mathrm{Im}\left[2\int_{z_0}^{z} \sqrt{\rho(s)}\,ds \right] = \mathrm{Im}\left[2\int_{z_0}^{\tau_c^{(n)}} \sqrt{\rho(s)}\,ds \right], \quad n=1,\ldots,N \right\}, \tag{A1}$$

where $\tau_c^{(n)}$, $n=1,N$ represent the crossing points and $\sqrt{\rho(s)}=\mathcal{E}(s)$ where $\mathcal{E}(s)$ is defined in Eq. (6). In order to construct Stokes lines, we choose a parametrization $\gamma(t)$ as

$$s=\gamma(t), \tag{A2}$$

with the condition $\gamma(t_0)=z_0$. We remark that the Stokes lines are independent of the chosen parametrization. In the following, we take one crossing point τ_c and we make calculation with only one crossing point. The formulas we determine later are valid for *each* crossing point. From Eq. (A1) and Eq. (A2), we obtain the following equation:

$$\mathrm{Im}\left[2\int_{t_0}^{t} \sqrt{\rho(\gamma(t))}\,\dot{\gamma}(t)\,dt \right] = \mathrm{Im}\left[2\int_{z_0}^{\tau_c} \sqrt{\rho(s)}\,ds \right] = \mathrm{const}, \tag{A3}$$

where $\dot{\gamma}(t)=d\gamma/dt$. Derivation of Eq. (A3) with respect to time implies that the function $\gamma(t)$ satisfies

$$\mathrm{Im}[\sqrt{\rho(\gamma(t))}\,\dot{\gamma}(t)]=0. \tag{A4}$$

Denoting $\gamma(t)=\gamma_r(t)+i\gamma_i(t)$, Eq. (A4) becomes

$$\dot{\gamma}_r(t)\mathrm{Re}[\sqrt{\rho(\gamma(t))}]+\dot{\gamma}_i(t)\mathrm{Im}[\sqrt{\rho(\gamma(t))}]=0. \tag{A5}$$

We can obtain solutions of Eq. (A5) by considering the following system of equations:

$$\dot{\gamma}_r(t)=\sigma\,\mathrm{Im}[\sqrt{\rho(\gamma(t))}],$$
$$\dot{\gamma}_i(t)=-\sigma\,\mathrm{Re}[\sqrt{\rho(\gamma(t))}], \tag{A6}$$

where $\sigma=\pm 1$. In the following, we choose $z_0=\tau_c$ since the crossing point belongs to the Stokes line. We start at the crossing point and we want to move along a Stokes line. However, the crossing point is an equilibrium point of Eq. (A6). The Stokes lines are the associated stable or unstable manifolds (depending on the choice of $\sigma=+1$ or $\sigma=-1$). In order to determine the stable and unstable directions, we consider the Taylor expansion of ρ written as

$$\rho(z)=\frac{d\rho}{dz}(z_0)(z-z_0)+O(z-z_0)^2. \tag{A7}$$

We define the real numbers r_0 and α such that $d\rho/dz(z_0)=r_0e^{i\alpha}$. By integrating we obtain

$$\int_{z_0}^{z} \sqrt{\rho(z)}\,dz=\frac{2}{3}\sqrt{r_0}e^{i\alpha/2}(z-z_0)^{3/2}+O(z-z_0)^2. \tag{A8}$$

Equation (A3) implies $\mathrm{Im}[e^{i\alpha/2}(z-z_0)^{3/2}]=0$. In terms of polar coordinates $(z-z_0)=re^{i\theta}$, we deduce that there are exactly three Stokes lines of directions θ given by

$$\theta=\frac{2}{3}k\pi-\frac{\alpha}{3}, \quad k=0,1,2\,. \tag{A9}$$

If we want to follow a Stokes line in a direction θ, we have to use *one* of the two choices of sign $\sigma=\pm 1$ in Eq. (A6), the one which makes that direction unstable. In the implementation of the algorithm, we solve Eq. (A6) with an initial condition located at a small distance of z_0 in the directions given by Eq. (A9).

[1] L.D. Landau, Phys. Z. Sowjetunion **2**, 46 (1932).
[2] C. Zener, Proc. R. Soc. London, Ser. A **137**, 696 (1932).
[3] A.M. Dykhne, Zh. Eksp. Teor. Fiz. **41**, 1324 (1962) [Sov. Phys. JETP **14**, 941 (1962)].
[4] J.P. Davis and P. Pechukas, J. Chem. Phys. **64**, 3129 (1976).
[5] J.-T. Hwang and P. Pechukas, J. Chem. Phys. **67**, 4640 (1977).
[6] M.V. Berry, Proc. R. Soc. London, Ser. A **429**, 61 (1990).
[7] A. Joye, H. Kuntz, and C.-Ed. Pfister, Ann. Phys. (N.Y.) **208**, 299 (1991).
[8] A. Joye, G. Mileti, and C.-Ed. Pfister, Phys. Rev. A **44**, 4280 (1991).
[9] K.-A. Suominen, B.M. Garraway, and S. Stenholm, Opt. Commun. **82**, 260 (1991).
[10] K.-A. Suominen and B.M. Garraway, Phys. Rev. A **45**, 374 (1992).
[11] K.-A. Suominen, Opt. Commun. **93**, 126 (1992).
[12] L. Allen and J.H. Eberly, *Optical Resonance and Two-Level Atoms* (Dover, New York, 1987).
[13] B.W. Shore, *The Theory of Coherent Atomic Excitation* (Wiley, New York, 1990).
[14] M.V. Berry, Proc. R. Soc. London, Ser. A **414**, 31 (1987).
[15] R. Lim and M.V. Berry, J. Phys. A **24**, 3255 (1991).
[16] M.V. Berry and R. Lim, J. Phys. A **26**, 4737 (1993).
[17] A. Joye, J. Phys. A **26**, 6517 (1993).
[18] K. Drese and M. Holthaus, Eur. Phys. J. D **3**, 73 (1998).
[19] N. Rosen and C. Zener, Phys. Rev. **40**, 502 (1932).

[20] Yu.N. Demkov and K. Kunike, Vestn. Leningr. Univ., Ser. 4: Fiz., Khim. **16**, 39 (1969).
[21] A. Bambini and P.R. Berman, Phys. Rev. A **23**, 2496 (1981).
[22] E.J. Robinson and P.R. Berman, Phys. Rev. A **27**, 1022 (1983).
[23] E.E. Nikitin and S.Ya. Umanskii, *Theory of Slow Atomic Collisions* (Springer-Verlag, Berlin, 1984).
[24] A. Bambini and M. Lindberg, Phys. Rev. A **30**, 794 (1984).
[25] F.T. Hioe, Phys. Rev. A **30**, 2100 (1984).
[26] F.T. Hioe and C.E. Carroll, Phys. Rev. A **32**, 1541 (1985).
[27] F.T. Hioe and C.E. Carroll, J. Opt. Soc. Am. B **2**, 497 (1985).
[28] C.E. Carroll and F.T. Hioe, J. Phys. A **19**, 3579 (1986).
[29] D.S.F. Crothers, J. Phys. B **11**, 1025 (1978).
[30] B.S. Nesbitt, D.S.F. Crothers, S.F.C. O'Rourke and P.R. Berman, Phys. Rev. A **56**, 1670 (1997).
[31] P.R. Berman, L. Yan, K.-H. Chiam, and R. Sung, Phys. Rev. A **57**, 79 (1998).
[32] S. Guérin, L.P. Yatsenko, and H.R. Jauslin, Phys. Rev. A **63**, 031403(R) (2001).
[33] L.P. Yatsenko, S. Guérin, and H.R. Jauslin, e-print quant-ph/0107065, http://xxx.lanl.gov
[34] M.V. Berry, Proc. R. Soc. London, Ser. A **392**, 45 (1984).
[35] N.V. Vitanov and K.-A. Suominen, Phys. Rev. A **59**, 4580 (1999).
[36] L.M. Garrido and F.J. Sancho, Physica (Amsterdam) **28**, 553 (1962).
[37] F.J. Sancho, Proc. Phys. Soc. London **89**, 1 (1966).
[38] K. Drese and M. Holthaus, Eur. Phys. J. D **5**, 119 (1999).
[39] J.H. Shirley, Phys. Rev. **138**, B979 (1965).
[40] H.R. Jauslin, S. Guérin, and S. Thomas, Physica A **279**, 432 (2000).